CrystEngComm

Accepted Manuscript

This is an *Accepted Manuscript*, which has been through the Royal Society of Chemistry peer review process and has been accepted for publication.

Accepted Manuscripts are published online shortly after acceptance, before technical editing, formatting and proof reading. Using this free service, authors can make their results available to the community, in citable form, before we publish the edited article. We will replace this *Accepted Manuscript* with the edited and formatted *Advance Article* as soon as it is available.

You can find more information about *Accepted Manuscripts* in the Information for Authors.

Please note that technical editing may introduce minor changes to the text and/or graphics, which may alter content. The journal's standard Terms & Conditions and the Ethical guidelines still apply. In no event shall the Royal Society of Chemistry be held responsible for any errors or omissions in this *Accepted Manuscript* or any consequences arising from the use of any information it contains.

ROYAL SOCIETY OF CHEMISTRY

www.rsc.org/crystengcomm

A Strategy Enlightened from the Observed Energetic-energetic Cocrystals of BTF: Cocrystallizing and Stabilizing Energetic Hydrogen-free Molecules with Hydrogenous Energetic Coformer Molecules

Xianfeng Wei, Yu Ma, Xinping Long, and Chaoyang Zhang*

Research Center of Energetic Materials Genome Science, Institute of Chemical Materials, China Academy of Engineering Physics (CAEP), P. O. Box 919-327, Mianyang, Sichuan 621900, China.

Abstract

Energetic-energetic cocrystals (EECCs) are promising alternatives to high-energy and low-sensitivity explosives, which is still challenging in the field of energetic materials due to their intrinsic energy-sensitivity contradiction (high energy usually companies high sensitivity). We propose a strategy to combine highly energetic but unstable hydrogen-free molecules with hydrogenous energetic molecules to form stable EECCs and maintain energy, enlightened by analyzing the crystal packing of all observed BTF-based EECCs. That is, in contrast to the pure BTF crystal that is very sensitive to mechanics and shock, the increased intermolecular hydrogen bonding consolidates the EECCs, exhibiting largely enhanced cohesive energy densities. And the hydrogen bonds are formed regardless of coformer molecular geometry, suggesting a large number of potential coformer molecules and EECCs. Moreover, the thermodynamics driving the EECC formation is discussed, and the increased lattice energy and increased entropy are thought to be the driving force to the EECCs. This strategy for consolidating crystal to stabilize unstable molecules by increasing intermolecular hydrogen bonding will renew the vital force for some highly energetic compounds that have been overlooked for a long time, due to their poor environmental compatibility.

CrystEngComm Accepted Manuscript

1 Introduction

Cocrystals are attracting increasing interest in the field of crystal engineering. In particular, energetic cocrystals are an emergent event and open up a beautiful prospect for tailor-making energetic materials by crystal engineering [1-13]. As a special group of materials, it is usually necessary to maintain high energy or avoid too much energy dilution, and it therefore requires that all cocrystal components are energetic. Accordingly, a binary cocrystal of this kind is called an energetic-energetic cocrystal (EECC). In most cases, these EECCs are made by arranging existing molecules, rather than synthesizing new compounds. Relative to pure components, the properties of cocrystals are usually traded off. However, there are sometimes some exceptions. One case is that cocrystallization can cause a higher packing density in contrast to both pure components. For example, the packing density of TNT/1-bromonaphthalene cocrystal (1.737 g/cm^3) is higher than those of both TNT (1.704 g/cm^3) and 1-bromonaphthalene (1.489 g/cm^3)[1]. The other is a recent excited work by Matzger et al, which evidenced that an EECC of TITNB/DADP can possess lower impact sensitivity than both pure TITNB and DADP by increasing intermolecular interactions[12]. These two exceptions are very important to enhance both energy and safety that are the two most important properties of energetic materials, motivating people to seek new better EECCs. Moreover, cocrystallization making the unstable stable implies that EECC will bring new vital force to some old energetic molecules, which possess an excellent energy property, but have not been thought to be useful and have been deserted for a long time, due to their vital disadvantages like very poor environmental adaptability (e.g. facile hydrolysis or high sensitivity to external stimuli).

Energetically, it is usually the enhanced intermolecular interactions that drive the cocrystal formation. In usual energetic crystals composed of C, H, N and O atoms, the main intermolecular interactions are of H···O, H···N, O···O and N···O interactions, and other interactions like N···N, C···O

CrystEngComm Accepted Manuscript

and C···N possess very few populations[14,15]. This should not be surprised in that H and O atoms usually surround molecular nuclear skeletons as the atoms of substituents, while C atoms usually and N and O atoms sometime compose of the skeletons. That is to say, the intermolecular interactions are usually conducted through the intermolecular contacts of O and H atoms (H···O and O···O contacts)[14-16]. Among H···O, H···N, O···O and N···O interactions, the former two belong to hydrogen bonding and are usually more energetically favorable than the latter two. In fact, it has been verified that hydrogen bond (HB) can consolidate the energetic crystals and make them insensitive to impact[14,15]. However, excessive H atoms are disadvantageous to increase energy density, because covalent H atoms are usually possess a lower mass density than O and N atoms, leading to a lower crystal packing density. This will cause a lower detonation velocity because the detonation velocity is directly proportional to the packing density[17]. At the same time, the excessive H atoms can make intermolecular interactions weak due to the weak intermolecular interactions among H atoms. Also, excessively high content of O usually weaken the molecular stability and intermolecular interactions. Consequently, the O/H ratio of energetic crystals should be necessarily appropriate.

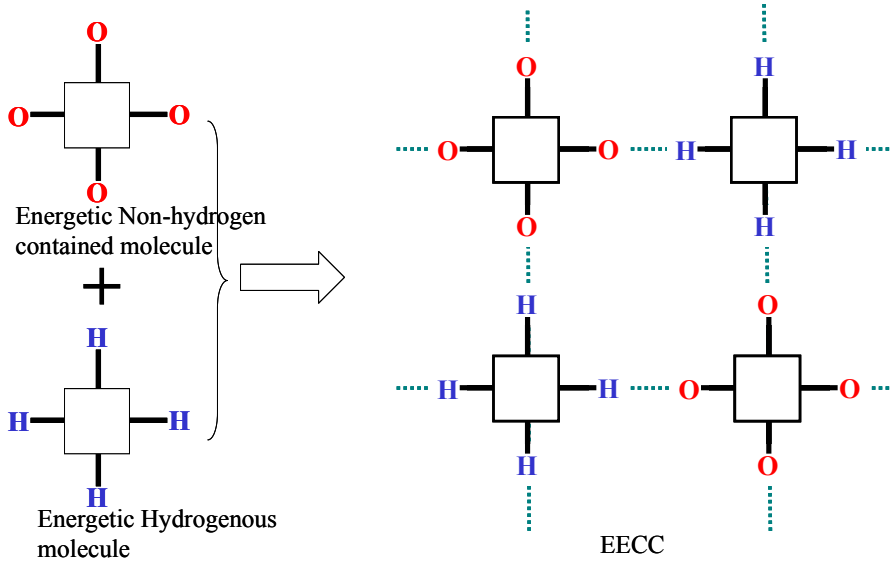

Fig. 1 Scheme showing the strategy to stabilize hydrogen-free energetic molecules by cocrystallizing with hydrogenous energetic molecules to form stable EECCs.

CrystEngComm Accepted Manuscript

As pointed out above, most of energetic-energetic cocrystallization proceeds from the existing energetic molecules. This possibly profits from utilizing numerous energetic molecules that have been synthesized already but have not been thought to be useful previously owing to their poor compatibility or stability. Among these overlooked molecules, there are an important group of hydrogen-free molecules. Many of these molecules such as HNB, ONC, DNF and DNOF feature high energy [18], making them the promising components to form high EECCs. That is, the excellence in energy of these compounds could be displayed in practice by the stabilizing effect of cocrystallization. On the other hand, these molecules, with high O contents and low stability, require to be stabilized by increasing intermolecular interactions like HB. Therefore, as illustrated in Fig. 1, it is a strategy to select fit energetic hydrogenous coformer molecules to maintain energy and stabilize these energetic hydrogen-free molecules. That is, to a certain extent, the disadvantages of low molecular stability could be overcome through cocrystallization, suggesting that it could make the highly energetic molecules that have ever been thought to be useless useful this time.

BTF is a typical hydrogen-free explosive and composed of C, N and O atoms[19]. In contrast to above-mentioned HNB, ONC, DNF and DNOF, BTF possesses similarly high sensitivity but better environmental adaptability and better controllability, and is therefore applied as a primary explosive[18]. From a viewpoint of molecular structure, BTF is similar to HNB, ONC, DNF and DNOF as O and N atoms compose of the external moiety of each molecule while C atoms compose of the internal moiety. Due to the requirement of oxygen balance of high explosives, the O/C ratio should remain appropriate to guarantee a heat release as enough as possible. In a word, BTF is a representative of hydrogen-free high explosives, and O atoms are always exposed around the molecules. Up to date, it has been reported seven BTF-based EECCs[6,8,11], possessing the largest population of all observed EECCs. Presumably, other hydrogen-free high-energy molecules can also be cocrystallized to form new

CrystEngComm Accepted Manuscript

EECCs as they possess similar molecular structures to BTF. If it is, the yield of EECCs will largely increase and some of them may be applicable.

Thereby, a systemic analysis of the crystal packing of all these BTF-based EECCs becomes crucial. Enlightened by the analysis, this work proposes a strategy to cocrystallize unstable energetic hydrogen-free molecules with energetic hydrogenous molecules to obtain energetic materials with tuned components, structures, properties and performances. That is, the O or H contents that cannot be tuned in a pure molecule can be tuned through cocrystallizing a hydrogen-free molecule with hydrogenous one.

2 Methodologies

2.1 Quantum Theory of Atoms in Molecule (QTAIM) Analyses.

QTAIM is useful tool to confirm the nonbonding interactions[20]. In QTAIM analyzing, the required wave functions of the single molecules and the molecular pairs extracted from crystals were calculated at the level of M062X/6-311+G (d,p) of density function theory[21]. The HB energy or the bond dissociation energy of HB (E_{HB}) was assessed by analyzing the electron density (ρ) at the bond critical points, by which the potential energy density (v) could be obtained. Then, E_{HB} was predicted using an empirical equation E_{HB}=-(1/2) v proposed by Espinosa et al [22]. All the electronic structure calculations were performed using package of Gaussian 09 [23].

2.2 Electrostatic Potential (ESP) Analyses.

The density function theory at the level of M062X/6-311+G (d,p) was also adopted to calculate ESP. The ESP on an isosurface of electron density (ρ) of 0.001 au was shown using GaussView 5.0.8.

2.3 Hirshfeld Surface Analyses.

Hirshfeld surface is a straightforward tool to understand intermolecular interactions[24-26]. Hirshfeld surfaces in a crystal were constructed in terms of electron distributions, calculated as the

CrystEngComm Accepted Manuscript

sum of spherical atom electron densities. The normalized contact distance (d_{norm}) was determined by d_i and d_e, the distances from the surface to the nearest atom interior and exterior to the surface respectively, and the van der Waals radii of the atoms, and represented by eq 1.

$$d_{norm} = \frac{d_i - d_i^{vdW}}{r_i^{vdW}} + \frac{d_e - r_e^{vdW}}{r_e^{vdW}} \quad (1)$$

d_{norm} enables the identification of the regions of particular importance to intermolecular interactions. That is to say, a Hirshfeld surface is composed of lots of points, and each point parametrized as (d_i, d_e) can provide information about related contact distances from it. The smaller $d_i + d_e$ suggests the closer atom-atom contact. Both d_i and d_e, were constrained in a range of 0 to 2.6 Å. Mapping these (d_i, d_e) points and considering their relative frequencies, one can get a two-dimensional (2D) fingerprint plot. For any symmetrically dependent molecule in any crystal, the fingerprint is unique. This is the base for identifying a crystal environment of a given molecule. The color mapping distinguishes the intensity of points, and the red and the blue represent the high and low intensities, respectively. Therefore, through the locations of (d_i, d_e) points and their relative frequencies discernible on the surface and the 2D fingerprint plot, we could ascertain the distances and intensities of these contacts. All the surfaces and fingerprint plots were created using CrystalExplorer3.0.57 and in this work, the surfaces were mapped over a d_{norm} range of −0.2 to 1.2 Å[27].

2.4 Lattice Energy and Cohesive Energy Density Calculations.

To study the driving force to EECC formation, PIXEL, based on density functional theory combined with semiempirical summations, was employed to calculate the lattice energy (E_c) and thereafter cohesive energy density (CED). The Pixel method is not feasible for the case of $Z'>2$. Fortunately, the largest Z' of the crystals discussed is 2, suggesting the availability of PIXEL in this work. CED is the energy when one mol volume solid (V_m) overcome the intermolecular force and vaporizes (E_{vap}), represented by $CED=E_{vap}/V_m$. In this article, we supposed $E_{vap}=E_c$. In general, the

CrystEngComm Accepted Manuscript

bigger CED suggests the stronger intermolecular interactions, as CED=E_c/V_m.

3 Results and Discussion

3.1 Molecular Structures

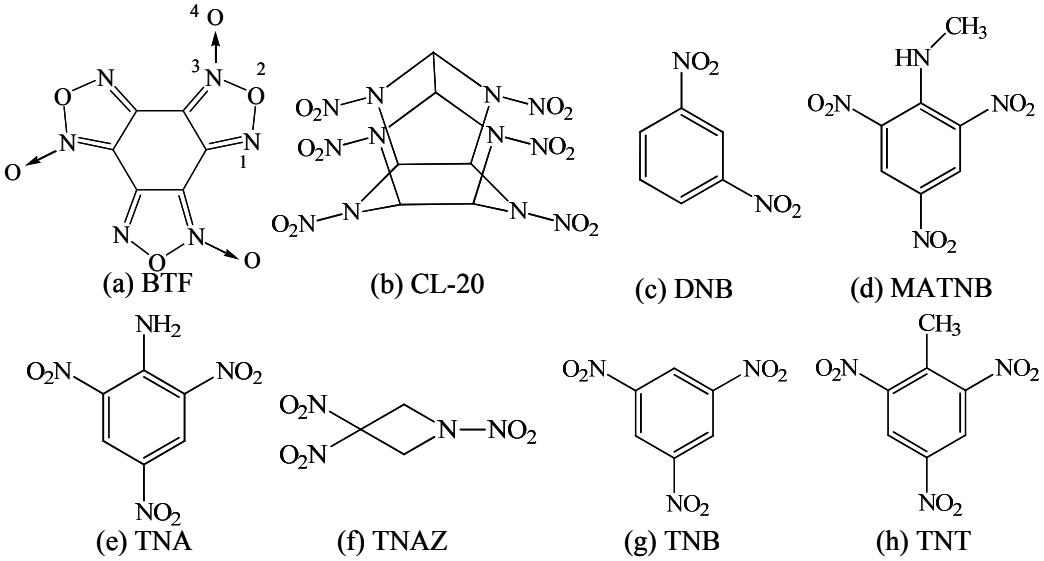

Fig. 2 Molecular structures of hydrogen-free BTF (a) and hydrogenous coformers (b-h). The numbers of BTF is employed to distinguish the atom kinds mentioned necessarily.

The molecular structures of hydrogen-free BTF and seven energetic hydrogenous coformer molecules are shown in Fig. 2, and the crystallographic information of the seven BTF-based cocrystals is listed in Table s1 of Electronic Supplementary Information (ESI). BTF is a planar conjugated molecule with a big π_{18}^{24} bond (18 atoms and 24 π-electrons) composed of all atoms in the molecule. As illustrated in Fig. 2(a), for BTF, it should be reasonable that the O and N atoms composing of the molecular peripheral moiety are the potential HB acceptors, due to their strong electronegativity. This can be verified by the ESP surface of BTF shown in Fig. 3(a): all the molecular margins are negatively charged, tending to accept HBs. It is interesting to find that all seven coformer molecules are hydrogenous (Figs 2(b)-(h)). These molecules are cage-shaped (CL-20), conjugated with all non-hydrogen atoms in the entire molecules (DNB, TNB and TNA), partly-conjugated (MATNB and TNT), or non-conjugated (TNAZ). The structural multiplicity of these coformer molecules suggests that the BTF can be cocrytallized with various energetic molecules, and H atoms are a key even

CrystEngComm Accepted Manuscript

though they are weak HB donors (through C-H). From the ESP surfaces of the seven coformer molecules in Figs 3(b)-(h), one can find the regions on which the H atoms are located are positively charged, with a tendency to be HB donors.

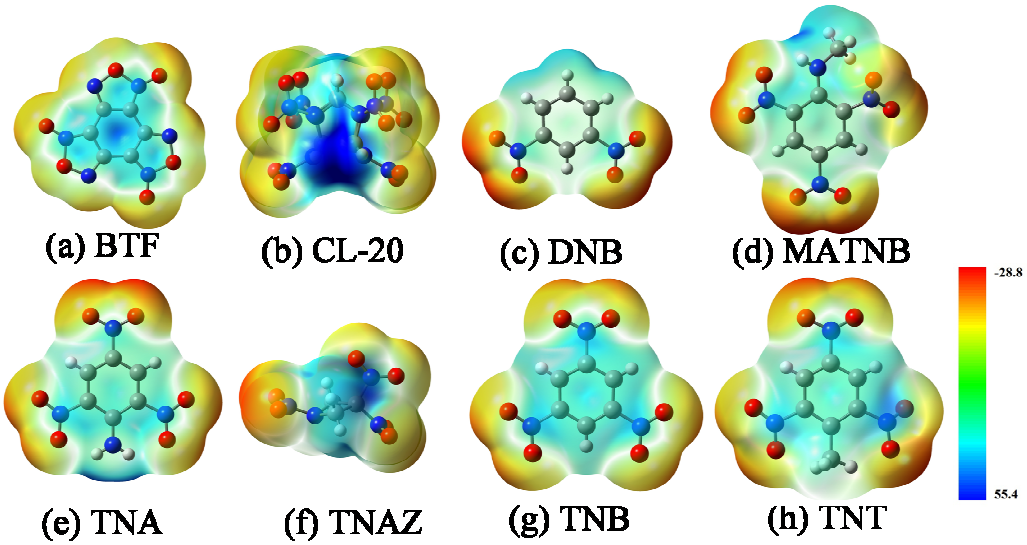

Fig. 3 ESP (in kcal/mol) of hydrogen-free BTF (a) and hydrogenous coformers (b-h) mapped onto the molecular surfaces of electronic density of 0.001 au. The grey, white, blue and red represent C, H, N and O atoms, respectively. These representations are considered in the following figures.

On the other hand, as demonstrated in Fig. 3(a), the benzene ring of BTF is positively charged, which is advantageous to interact with the negatively charged atoms of the seven coformer molecules, for example, the O atoms of nitro groups shown in Figs 3(b)-(h). These interlaced electrostatic interactions plus HBs consolidate the BTF-based EECCs, exhibiting greatly increased CED in contrast to the pure BTF crystal. This will be discussed later.

3.2 Intermolecular HB in Crystal Packing.

The HBs exist in the BTF-based EECCs, greatly different from the pure BTF crystal without HB. Because the intermolecular HBs between BTF and coformer molecules is a key to understand the crystal packing variation caused by cocrystallization, we only focus on them and discuss them through geometry analyses, QTAIM confirmation and Hirshfeld surface analyses in this section. By the way, from all the intermolecular HBs of the EECCs shown in Fig. s1 of ESI, we can find these HBs can exist not only between BTF and the coformer molecules, but also between the coformer molecules

CrystEngComm Accepted Manuscript

themselves.

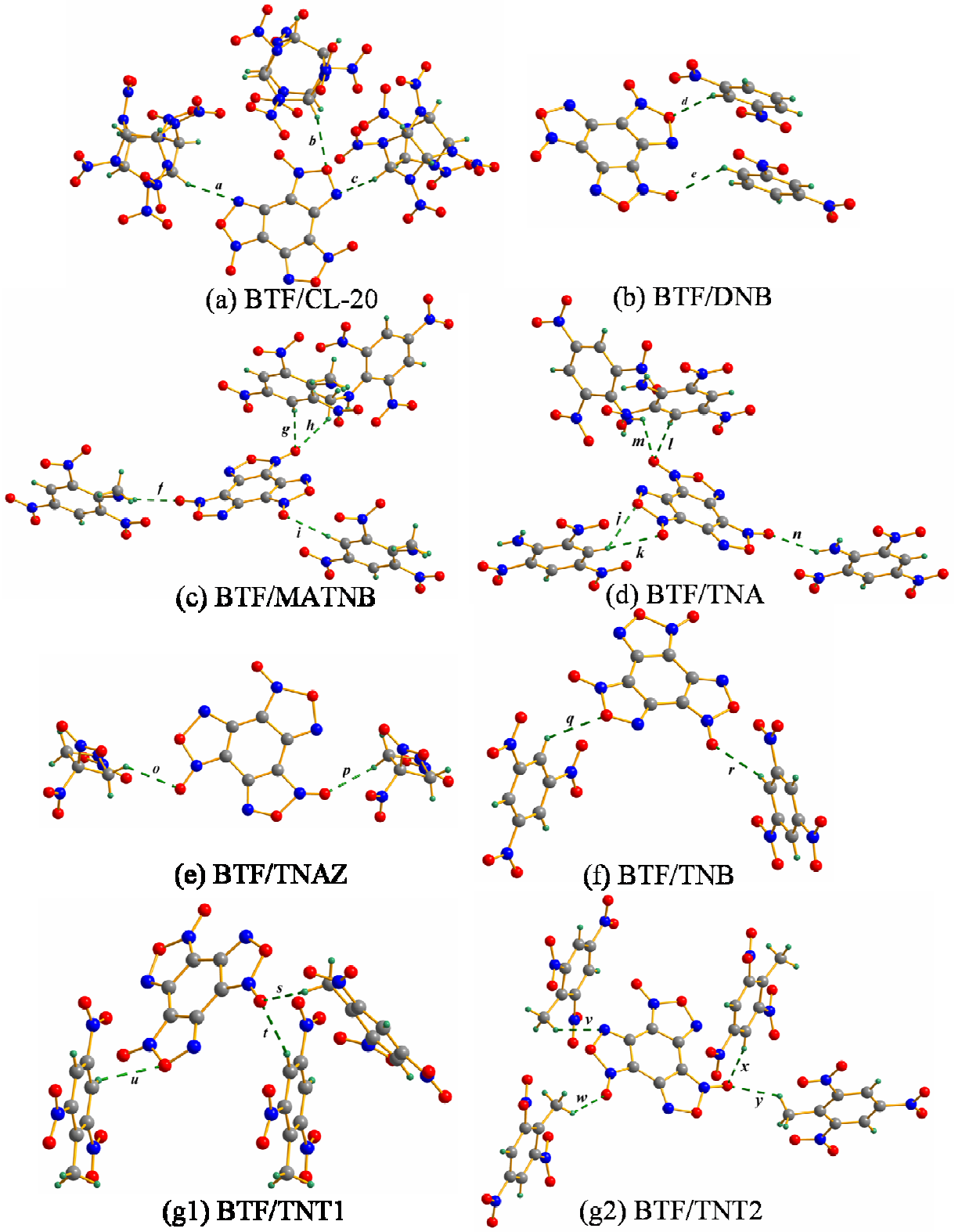

Fig. 4 HBs Between hydrogen-free BTF and hydrogenous coformers in the BTF-based EECCs extracted by those between a BTF molecule and its surrounding coformer molecules and denoted by green dash. The cocrystal of BTF/TNT possesses Z′=2, therefore the HBs are illustrated by (g1) and (g2) separately. Low case letters a-y are the numbers of HBs, corresponding to the letters in Table s2 of ESI.

CrystEngComm Accepted Manuscript

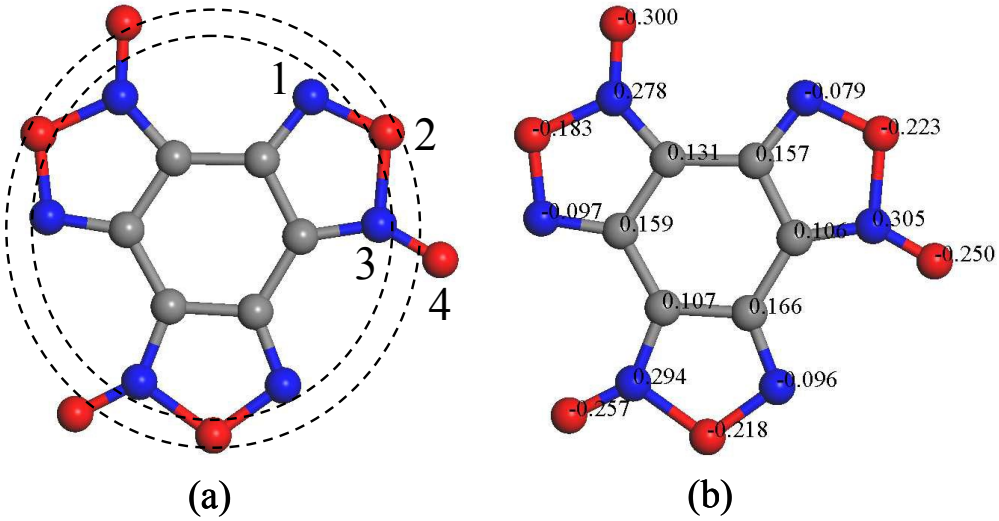

Fig. 5 Plot showing distances from the atoms to the centroid of BTF molecule (a) and Mulliken charges (unit in e) on atoms (b). The numbers is used to distinguish the atom kinds.

Fig. 4 illustrates the HBs and their details of geometry, and their QTAIM analyses are listed in Table s2 of ESI. It is interesting to find that the HBs exist in all seven EECCs as expected, even though they are always weak, usually with several kJ/mol of E_{HB} shown in Table s2 of ESI. With respect to the BTF molecule, three kinds of atoms including acyl O atoms, and O and N atoms on furazan ring, numbered as 4, 2 and 1 in Fig. 2(a), respectively, are potential HB acceptors. In Fig. 4, we find the three kinds of HBs as expected, in which 4, 2 and 1 act as HB acceptors. The most HBs are formed by 4 and coformer-H atoms (17 out of 25) when BTF is cocrystallized with DNB, MATNB, TNA, TNAZ, TNB and TNT. This should be reasonable that 4 are located on the most external of the BTF molecule, with a highest probability to contact neighboring molecules in crystal. The HBs between 2 and the H atoms of the CL-20, DNB, TNA, TNB and TNT molecules take the second place (5 out of 25). The remaining HBs are formed by 1 and the H atoms of the CL-20 and TNT molecules (3 out of 25). That is, the amounts the three kinds of HBs in the seven BTF-based EECCs decrease in an order of 4, 2 and 1. This should be strongly related with two factors indicated in Fig. 5. One is the distance between the HB acceptor atoms to the molecular centroid. As pointed out above, the farther distance suggests the higher probability to contact neighboring molecules and

CrystEngComm Accepted Manuscript

form HBs. Fig. 5(a) illustrates the distances in an increasing order of 4, 3=2 and 1. The other is the amount and sign of the charges on the HB acceptor atoms: the more negative charges, the higher ability to build HBs. Fig. 5(b) shows that the negative Mulliken charges (calculated at the level of PBE/DNP using Dmol^3 package) decrease from 4 to 2 and 1, and the charges on 3 is positive. Regarding to these charges and distances, we can confirm that a tendency to form HBs reduces from 4 to 2 and 1, in agreement with above order of HB quantities.

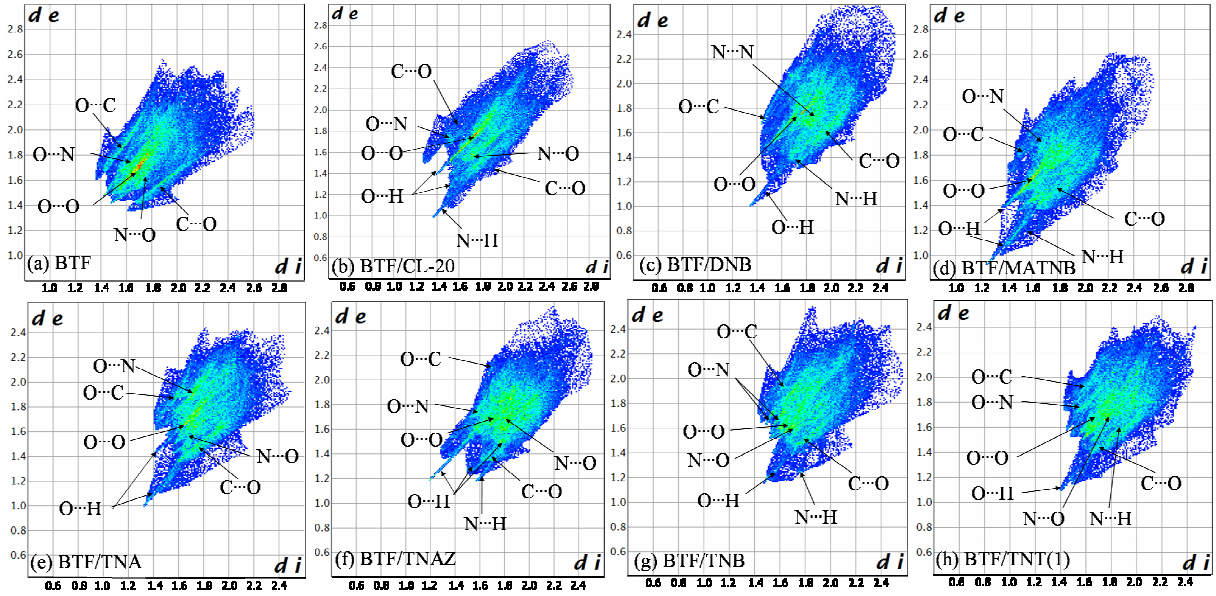

Fig. 6 Two-dimensional fingerprint plots of BTF molecules in crystals.

Hirshfeld surface and two-dimensional fingerprint plot derived from it are useful tools to explore intermolecular interactions. Converting the data of Hirshfeld surfaces shown in Fig. s3 of SI, we can obtain related two-dimensional plots of BTF molecules in the pure BTF crystal and the seven BTF-based EECCs in Fig. 6. From Figs 6(b) to 6(h), we can readily find that there is at least one spike on bottom left on each plot, in contrast to no spike of pure BTF in Fig. 6(a). Usually, the spikes on bottom left of the two-dimensional plot suggest the HBs between the assigned molecule and its neighbors, and the shorter distance of the spike to the origin of coordinate suggests the

CrystEngComm Accepted Manuscript

stronger HB [24-26]. That is to say, evident HBs are formed in EECCs, even though they are all weak, similar to the cases of general CHON explosive crystals[14-16]. Besides HBs, the O···O, C···O and N···O contacts are dominant in the pure BTF crystal and the BTF-based EECCs. The O···O interactions are attributed to the contacts between O atoms of the BTF molecules and nitro O atom of the coformer molecules. While, the C···O and N···O contacts are strongly related with the interactions between the electron-rich NO_2 of the coformer molecules and the electron-lack benzene ring of the BTF molecule (or called the n-π electronic interactions), and the π-π interactions due to π-structures in both the BTF molecule and most of coformer molecules including DNB, MATNB, TNA, TNB and TNT.

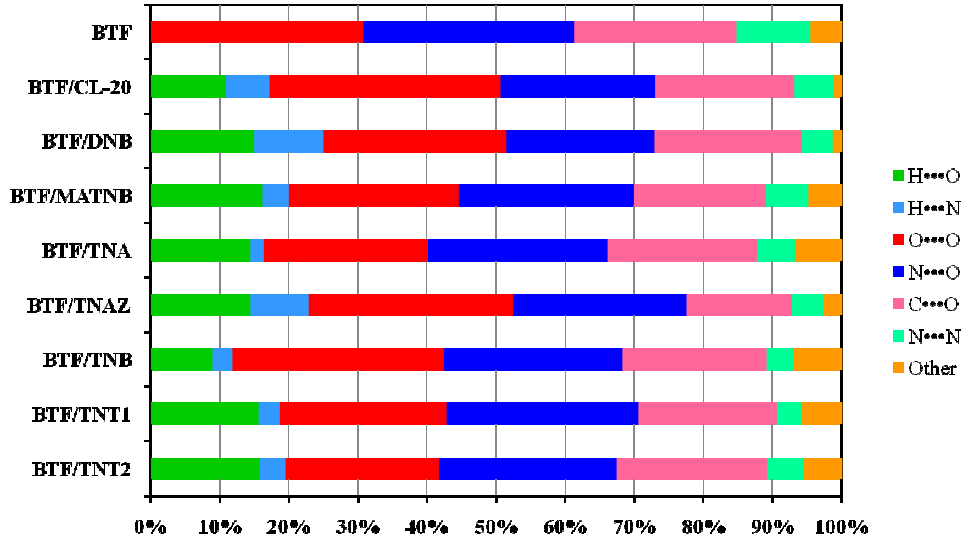

Fig. 7 Populations of the close interatomic contacts of BTF molecules in crystals.

To be more straightforward, we compare the populations of close contacts of BTF molecules involved in different crystals in Fig. 7, and we can find that the evident difference is the HB formation in the EECCs by O···H and N···H contacts. This is in agreement with above QTAIM analyses and conformation. From the figure, one can see that the HB populations are within 12 and 25 %. Relative to the pure BTF crystal, the populations of HBs in the EECCs increase at the cost of the reduction of the populations of O···O and N···N contacts. In addition, the O···O, C···O and

CrystEngComm Accepted Manuscript

N···O contacts are always predominant in all crystals.

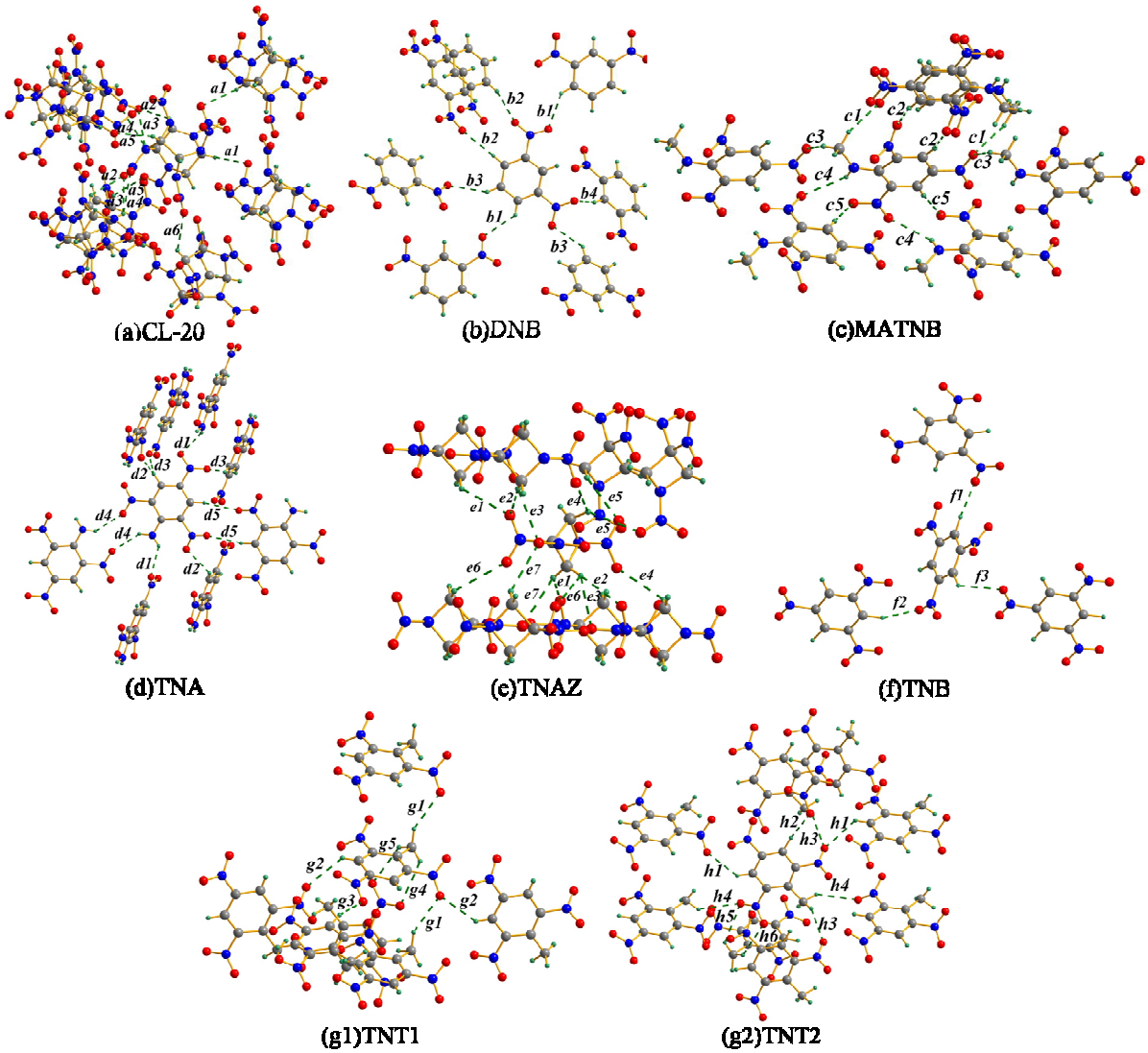

Fig. 8 HBs in pure crystals of hydrogenous coformers extracted by those between a central molecule and its neighbors and denoted by green dash. TNT possesses Z′=2, therefore the HBs are illustrated by (g1) and (g2) separately. Low case letters a1-h6 are numbers of HBs, corresponding to letters in Table s3 of ESI.

Naturally, the HBs in the pure coformer crystals will be considered. This is largely attributed to that the cocrystallization is a process involving first the HB dissociation of pure coformer crystals and then the HB formation in cocrystals. Therefore, the HBs in the pure coformer crystals were also analyzed and their strengths were compared with those in EECCs. Fig. s2 of ESI exhibits all HBs in the pure coformer crystals. Fig. 8 illustrates the HBs around a central coformer molecule. In

CrystEngComm Accepted Manuscript

combination with the details of geometry and QTAIM analyses of pure coformer crystals in Table s3 of ESI, we can come to a conclusion that the HBs in pure coformer crystals are similar to those in the EECCs. Firstly, apart from some intermolecular HBs in MATNB (c4 in Fig. 8(c)) belonging to N-H···O, the remaining is of C-H···O. As a matter of fact, this N-H···O interaction is also found in the interactions between BTF and MATNB molecules of their cocrystal (f in Fig. 4(c)). Different from EECCs, there is no C-H···N interactions in the pure coformer crystals.

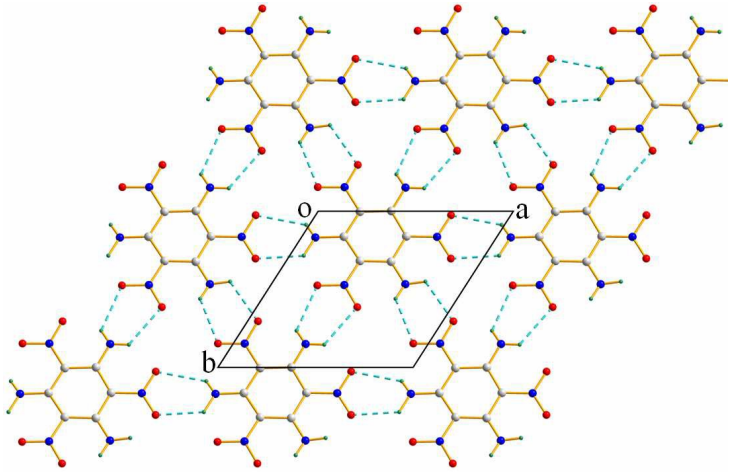

Fig. 9 HBs in the layers of TATB crystal.

Secondly, as illustrated in Fig. 8, only a part of potential HB acceptors (O atoms) and donors (H atoms) take part in the HB formation. That is, the efficiency of HB formation is not high. This is far from the case of a famous insensitive explosive TATB[29]. In the TATB crystal, as shown in Fig. 9, all the surrounding atoms contribute to the HBs, i.e., the efficiency of 100 %. The low efficiency of HB formation can also be found in EECCs as a large part of potential HB acceptors and donors do not contribute to HBs, as illustrated in Fig. 4. In general, it is thought that the stronger intermolecular interactions leads to the lower sensitivity to external stimuli, in that the break of intermolecular interactions is deemed as the first step to final combustion or detonation by molecular dissociation and hot spot formation and growth[30-33]: the stronger intermolecular

CrystEngComm Accepted Manuscript

interactions suggests the difficult bread. Because HB is usually energetically favored than other intermolecular interactions like O···O, C···O and N···O [16], the sensitivity of these BTF-based EECCs is expected to be improved in contrast to the pure BTF. However, the EECCs' sensitivity is expected to be much higher than that of TATB, due to the low efficiency of HB formation crystal packing and largely inferior molecular stability of BTF.

Table 1. The average H···A distance and E_{HB} of BTF-based EECCs and pure conformer crystals.

Explosives	H···A, Å		E_{HB}, kJ/mol	
	EECC	conformer crystal	EECC	conformer crystal
BTF/CL-20	2.640	2.655	4.8	5.5
BTF/DNB	2.617	2.628	5.3	4.7
BTF/MATNB	2.494	2.603	5.9	5.3
BTF/TNA	2.611	2.485	5.2	6.6
BTF/TNAZ	2.795	2.705	3.8	4.6
BTF/TNB	2.751	2.385	3.6	8.3
BTF/TNT1	2.691	2.592	4.5	5.8
BTF/TNT2	2.585	2.632	5.5	5.3

In final, we compare HBs in the two classes of crystals by averaging H···A (HB acceptor) distances and E_{HB}, and list them in Table 1. Even though there are relatively large H···A distance and E_{HB} differences between the BTF/TNB EECC and pure TNB crystal, as a whole, these differences are usual small. In summary, the HBs in the BTF-based EECCs and the pure coformer crystals are similar. Because the selected solvents in which both coformers have close solubility are crucial for EECC formation by solvent evaporation, it requires that coformer possesses close intermolecular interaction strength to BTF. As pointed before, the intermolecular interactions in the BTF crystal is weak, suggesting that the weak HBs in pure coformer crystals are understandable. Accordingly, if we want cocrystallize BTF with a coformer with stronger intermolecular interactions, for example, TATB, other cocrystallization methods apart from solvent evaporation should be considered, because TATB is very low soluble in any common solvent [18].

Relative to the pure BTF crystal, the HBs strengthen the intermolecular interactions since that

CrystEngComm Accepted Manuscript

HB is usually energetically favored than other intermolecular interactions like O···O, C···O and N···O, which are dominant in the BTF crystal. As expected, the CEDs of the EECCs in Fig. 10 are largely enhanced. It shows that the introduction of hydrogenous coformer molecules to cocrystallize with hydrogen-free BTF can increase its stability by increasing interactions. This is useful to increase the safety of energetic materials. For example, recently found TITNB/DADP possesses lower impact sensitivity than both pure TITNB and DADP by increasing intermolecular interactions[12].

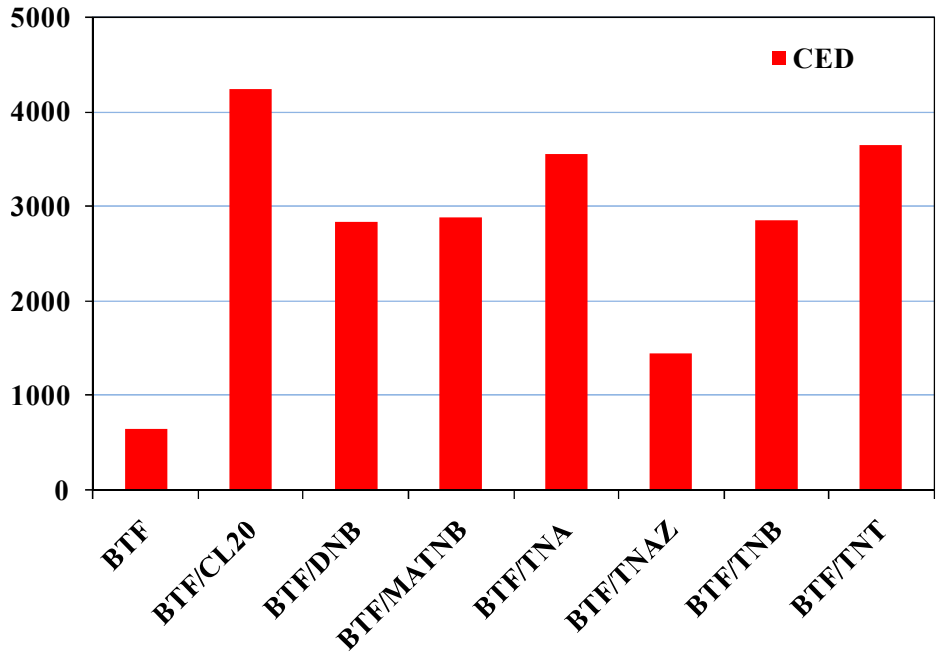

Fig. 10 Coherent energy density (CED) of the BTF crystal and the seven BTF-based EECCs.

Table 2. Energy of EECC formation (ΔE, unit in kJ/mol).

EECC	BTF/CL-20	BTF/DNB	BTF/MATNB	BTF/TNA	BTF/TNAZ	BTF/TNB	BTF/TNT
ΔE	-2.5	-5.8	-3.5	-3.9	-1.6	-4.7	-2.3

As to the thermodynamics driving the BTF-based EECCs formation, we first consider the lattice energy change after cocrystallization, the energy of EECC formation (ΔE), by Pixel calculations. That is, $\Delta E=E_{EECC}-(E_{C1}+E_{C2})$, where E_{EECC}, E_{C1} and E_{C2} are the lattice energy of the

CrystEngComm Accepted Manuscript

EECC and pure coformer crystals, respectively. Interestingly, it is found in Table 2 that the formation of all BTF-based EECCs is thermodynamically favored regarding to the negative ΔE. Moreover, to be more accurate, we should employ Gibbs free energy change (ΔG=ΔH-TΔS) to consider the thermodynamics in the EECC formation at a constant temperature and a constant pressure. Even though it is difficult to calculate free energy change (ΔG), we can also predict it should be negative as follows. On the condition of crystallization, enthalpy change (ΔH) is almost equal to ΔE, which are negative according to the calculated values in Table 2, and the entropy change (ΔS) should be positive due to the increase of mixing degree. The negative ΔH subtract the positive TΔS to get negative ΔG, suggesting a spontaneous process for forming the BTF-based EECC.

3.3 Enlightenment from the Observed BTF-based EECCs

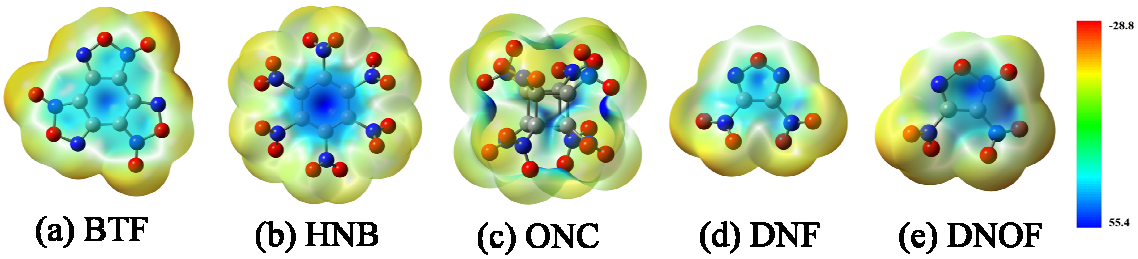

Fig. 11 ESP of hydrogen-free BTF, HNB, ONC, DNF, DNOF, and mapped onto the molecular surfaces of electronic density of 0.001 au.

As pointed out above, many hydrogen-free explosives such as HNB, ONC, DNF and DNOF feature high energy but low stability[18]. Similar to BTF, as demonstrated in Fig. 11, the externals of these explosive molecules are negatively charged, supplying an advantage to form HBs and increase intermolecular interactions. If we can cocrystallize these molecules with energetic hydrogenous molecules to form high EECCs, these unstable molecules might be stabilized to a certain extent. That is, their potentials of high energy might be brought into practice. Obviously, some techniques like choices of temperature and solvent to prevent these hydrogen-free energetic compounds from

CrystEngComm Accepted Manuscript

decomposition or hydrolysis should be considered.

4. Conclusions

Nowadays, the explosive with high energy density and low sensitivity is becoming an object in developing new energetic materials. EECCs are the potential alternatives as they can maintain energy density or avoid too much energy dilution. Meanwhile their components could be stabilized by cocrystallization. This will offer a chance to some highly energetic but unstable explosives like hydrogen-free HNB, ONC, DNF and DNOF, which have already been thought to be no use for a long time.

This work verifies and exemplifies this possibility by systemically analyzing the crystal packing of all observed BTF-based EECCs, in which BTF is an available but very sensitive explosive to impact or shock. As results, we find that the BTF molecule is readily combined with hydrogenous coformer molecules through intermolecular HBs, regardless of the geometry structures of the coformer molecules. Relative to the pure BTF crystal, the enhanced intermolecular interactions in the BTF-based EECCs lead to much higher CEDs. Compared the HBs in the EECCs and pure coformer crystals, we find that they are slightly different from one another. Moreover, by means of a series of semi-empirical Pixel calculations on lattice energy, it is predicted that the EECC formation is energetically favored. Also, the role of entropy increases should not be overlooked in driving the EECC formation.

In summary, a strategy to develop high-energy and low-sensitivity energetic materials is proposed to cocrystallize hydrogen-free high-energy molecules with hydrogenous energetic molecules to form EECCs.

Abbreviations

BTF benzotrifuroxan

CrystEngComm Accepted Manuscript

CL-20	2,4,6,8,10,12-hexanitro-2,4,6,8,10,12-hexaazaisowurtzitane
DADP	3,3,6,6-Tetramethyl-1,2,4,5-tetroxane
DNB	1,3-Dinitrobenzene
DNF	3,4-dinitro-1,2,5-oxadiazole
DNOF	2-oxide-3,4-dinitro-1,2,5-oxadiazole
HNB	hexanitrobenzene
MATNB	1-methyl-amino-2,4,6-trinitrobenzene
ONC	octanitrocubane
TITNB	1,3,5-triiodo-2,4,6-trinitrobenzene
TNA	2,4,6-trinitroaniline
TNAZ	1,3,3-trinitroazetidine
TNB	1,3,5-trinitrobenzene
TNT	2,4,6-trinitrotoluene

Corresponding Author

Prof. Chaoyang Zhang, e-mail: chaoyangzhang@caep.cn.

Acknowledgment

We are greatly grateful for the financial support from the Science and Technology Fund of CAEP (2012A0302013), the Science and Technology Innovation Fund of ICM (KJCX-201305) and the National Natural Science Foundation of China (21173199).

Electronic Supplementary information

It includes crystallographic information of 8 crystals, HBs in seven BTF-based EECCs and seven pure coformer crystals, and Hirshfeld surfaces of BTF molecules involved in pure BTF crystal and the seven BTF-based EECCs.

References and Notes

1 K. B. Landenberger and A. J. Matzger, *Cryst. Growth Des*. 2010, 10, 5341-5347.

2 O. Bolton and A. J. Matzger, *Angew. Chem. Int. Ed*. 2011, 50, 8960-8963.

3 K. B. Landenberger and A. J. Matzger, *Cryst. Growth Des*. 2012, 12, 3603-3609.

4 O. Bolton, L. R. Simke, P. F. Pagoria and A. J. Matzger, *Cryst. Growth Des*. 2012, 12,

CrystEngComm Accepted Manuscript

4311-4314.

5 C. Guo, H. Zhang, X. Wang, X. Liu and J. Sun, *J. Mater. Sci.,* 2012, 48, 1351-1357.

6 Z. W. Yang, H. Z. Li, X. Q. Zhou, C. Y. Zhang, H. Huang, J. S. Li and F. D. Nie, *Cryst. Growth Des*. 2012, 12, 5155-5158.

7 D. Millar, H. Maynard-Casely, D. Allan, A. Cumming, A. Lennie, A. Mackay, I. Oswald, C. Tang and C. Pulhama, *CrystEngComm*, 2012, 14, 3742-3749.

8 H. Zhang, Z. Cuo, X. Wang, J. Xu, X. He, Y. Liu, X. Liu, H. Huang and J. Sun, *Cryst. Growth Des*. 2013, 15, 679-687.

9 K. B. Landenberger, O. Bolton and A. J. Matzger, *Angew. Chem. Int. Ed*. 2013, 52, 6468-6471.

10 C. Zhang, Z. Yang, X. Zhou, C. Zhang, Yu. Ma, J. Xu, Q. Zhang, F. Nie and H. Li, *Cryst. Growth Des.,* 2014, 14, 3923-3928.

11 Z. Yang, Y. Wang, J. Zhou, H. Li, H. Huang and F. Nie, *Propel, Explos, Pyrotech*. 2014, 39, 9-13.

12 K. B.Landenberger, O. Bolton and A. J. Matzger, *J. Am. Chem. Soc*. 2015, 137, 5074-5079.

13 J. C. Bennion, A. McBain, S. F. Son and A. J. Matzger, *Cryst. Growth Des.* 2015, 15, 2545-2549.

14 Y. Ma, A. Zhang, C. Zhang, D. Jiang, Y. Zhu and C. Zhang, *Cryst. Growth Des*, 2014, 14, 4703-4713.

15 Y. Ma, A. Zhang, X. Xue, D. Jiang, Y. Zhu and C. Zhang, *Cryst. Growth Des.*, 2014, 14, 6101-6114.

16 C. Zhang, X. Xue, Y. Cao, J. Zhou, A. Zhang, H. Li, Y. Zhou, R. Xu and T. Gao, *CrystEngComm*, 2014, 16, 5905-5916.

17 M. J. Kamlet and S. J. Jacobs, *J. Chem.Phys*. 1968, 48, 23-35.

18 H. Dong and F. Zhou, *High Energetic Explosives and Relatives*, Science Press, Beijing, 1994.

19 H. H. Cady, A. C. Larson and D. T. Cromer, *Acta Crystallogr*, 1966, 20, 336.

20 R. Bader, *Atoms in Molecules: A Quantum Theory*. *The International Series of Monographs of Chemistry*; J. Halpen and M. L. H. Green, Eds.; Clarendon Press: Oxford, 1990.

21 Y. Zhao and D. G. Truhlar, *Theor. Chem. Acc.,* 2008, 120, 215-241.

22 E. Espinosa and E. Molins, *J. Chem. Phys*. 2000, 113, 5686-5694.

23 M. J. Frisch, et al. Gaussian 09, Revision B.01, Gaussian, Inc., Pittsburgh PA, 2009.

24 M. A. Spackman and P. G. Byrom, *Chem. Phys. Lett*. 1997, 267, 215-220.

CrystEngComm Accepted Manuscript

25 M. A. Spackman and J. J. McKinnon, *CrystEngComm* 2002, 4, 378-392.

26 J. J. McKinnon, D. Jayatilaka and M. A. Spackman, *Chem. Commun*. 2007, 37, 3814-3816.

27 S. K. Wolff, D. J. Grimwood, J. J. McKinnon, D. Jayatilaka and M. A. Spackman, Crystal Explorer 3.0; University of Western Australia: Perth, Australia, 2009.

28 A. Gavezzotti, *CrystEngComm*, 2008, 10, 389-397.

29 H. H. Cady and A. C. Larson, *Acta Crystallogr.* 1965, 18, 485-496.

30 E. A. Zhurova, V. V. Zhurov and A. A. Pinkerton, *J. Am. Chem. Soc.* 2007, 129, 13887-13893.

31 E. A. Zhurova, A. I. Stash, V. G. Tsirelson, V. V. Zhurov, E. V. Bartashevich, V. A. Potemkin and A. A. Pinkerton, *J. Am. Chem. Soc.* 2006, 128, 14728-14734.

32 E. A. Zhurova, V. G. Tsirelson, A. I. Stash and A. A. Pinkerton, *J. Am. Chem. Soc.* 2002, 124, 4574-4575.

33 E. A. Zhurova, V. G. Tsirelson, A. I. Stash, M. V. Yakovlev and A. A. Pinkerton, *J. Phys. Chem. B* 2004, 108, 20173-20179.

CrystEngComm Accepted Manuscript

TOC

A Strategy Enlightened from the Observed Energetic-energetic Cocrystals of BTF: Cocrystallizing and Stabilizing Energetic Hydrogen-free Molecules with Hydrogenous Energetic Coformer Molecules

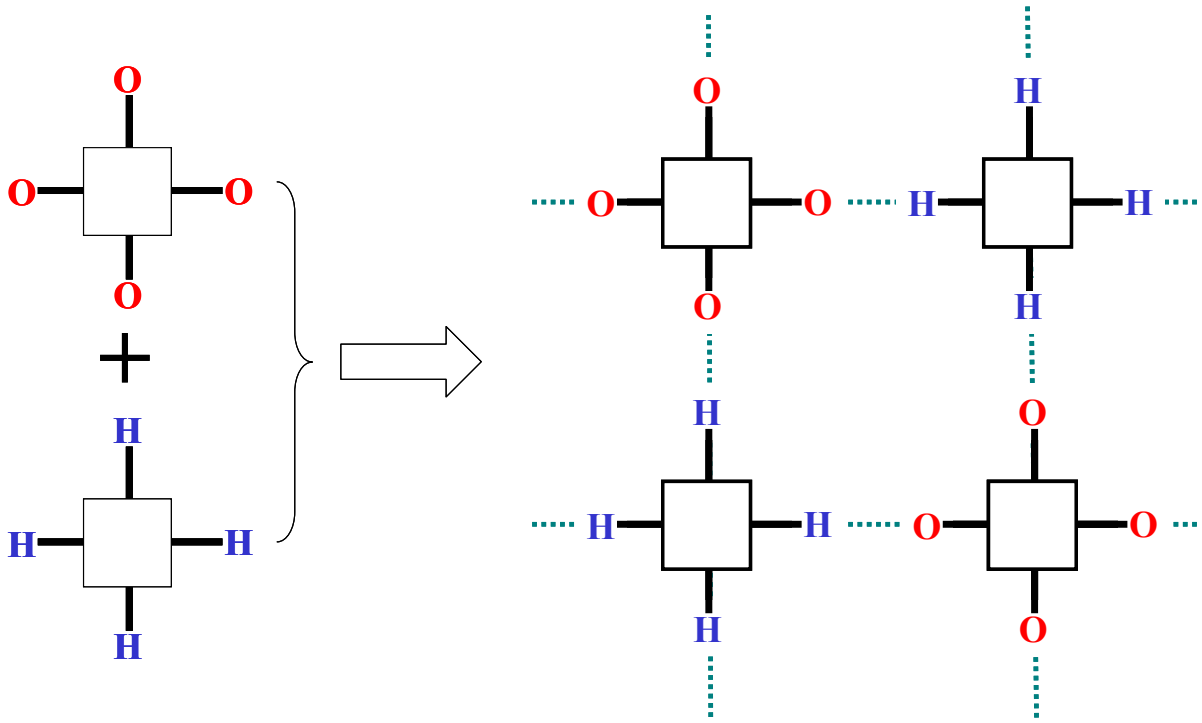

CrystEngComm Accepted Manuscript

A Strategy Enlightened from the Observed Energetic-energetic Cocrystals of BTF: Cocrystallizing and Stabilizing Energetic Hydrogen-free Molecules with Hydrogenous Energetic Coformer Molecules

Xianfeng Wei, Yu Ma, Xinping Long, and Chaoyang Zhang*

Research Center of Energetic Materials Genome Science, Institute of Chemical Materials, China Academy of Engineering Physics (CAEP), P. O. Box 919-327, Mianyang, Sichuan 621900, China.

Electronic Supporting Information (ESI)

Table of Contents

CrystEngComm Accepted Manuscript

S1. Crystallographic information of BTF and seven BTF-based Cocrystals discussed.

Table s1. Crystallographic information of crystals discussed.

Explosives	BTF[1]	BTF/CL-20[2]	BTF/DNB[3]	BTF/MATNB[4]
Refcode	BZOFOX	PEHSUS	-	GEXMON
Formula	$C_6N_6O_6$	$C_{12}H_9N_{18}O_{18}$	$C_{12}H_4N_8O_{10}$	$C_{13}H_6N_{10}O_{12}$
Symmetry	Orthorhombic	Orthorhombic	monoclinic	monoclinic
Space group	$Pna2_1$	$P2_12_12_1$	$P2_1/c$	$P2_1/c$
a(Å)	6.923(1)	9.275(5)	9.362	9.332(<1)
b(Å)	19.516(1)	11.946(7)	13.005	12.604(<1)
c(Å)	6.518(1)	21.577(12)	14.911	15.476(<1)
α(°)	90.00	90.00	90.00	90.00
β(°)	90.00	90.00	96.07	90.62(<1)
γ(°)	90.00	90.00	90.00	90.00
V(Å^3)	880.642	2390.713	1609.14	1820.169
Z	4	4	4	4
Density(g/cm^3)	1.901	1.926	1.735	1.804
Temperature (K)	RT	RT	RT	145
Ratio		1:1	1:1	1:1
Explosives	BTF/TNA[4]	BTF/TNAZ[4]	BTF/TNB[4]	BTF/TNT[4]
Refcode	GEXMIH	ZEVNUL	GEXMED	GEXMAZ
Formula	$C_{12}H_4N_{10}O_{12}$	$C_9H_4N_{10}O_{12}$	$C_{12}H_3N_9O_{12}$	$C_{13}H_5N_9O_{12}$
Symmetry	$P2_1/c$	$P\bar{1}$	$P2_1/c$	$P\bar{1}$
Space group	monoclinic	triclinic	monoclinic	triclinic
a(Å)	9.402(<1)	6.747(<1)	9.549(<1)	9.338(<1)
b(Å)	12.675(<1)	10.389(<1)	12.567(<1)	12.896(<1)
c(Å)	14.327(<1)	12.348(1)	14.454(<1)	14.729(<1)
α(°)	90.00	70.75(<1)	90.00	88.51(<1)
β(°)	97.41(<1)	88.77(<1)	99.53(<1)	84.16(<1)
γ(°)	90.00	80.12(<1)	90.00	88.94(<1)
V(Å^3)	1693.105	804.394	1710.617	1763.537
Z	4	2	4	4
Density(g/cm^3)	1.884	1.834	1.806	1.805
Temperature (K)	135	RT	RT	145
Ratio	1:1	1:1	1:1	1:1

CrystEngComm Accepted Manuscript

S2. HBs in seven BTF-based EECCs and seven pure coformer crystals.

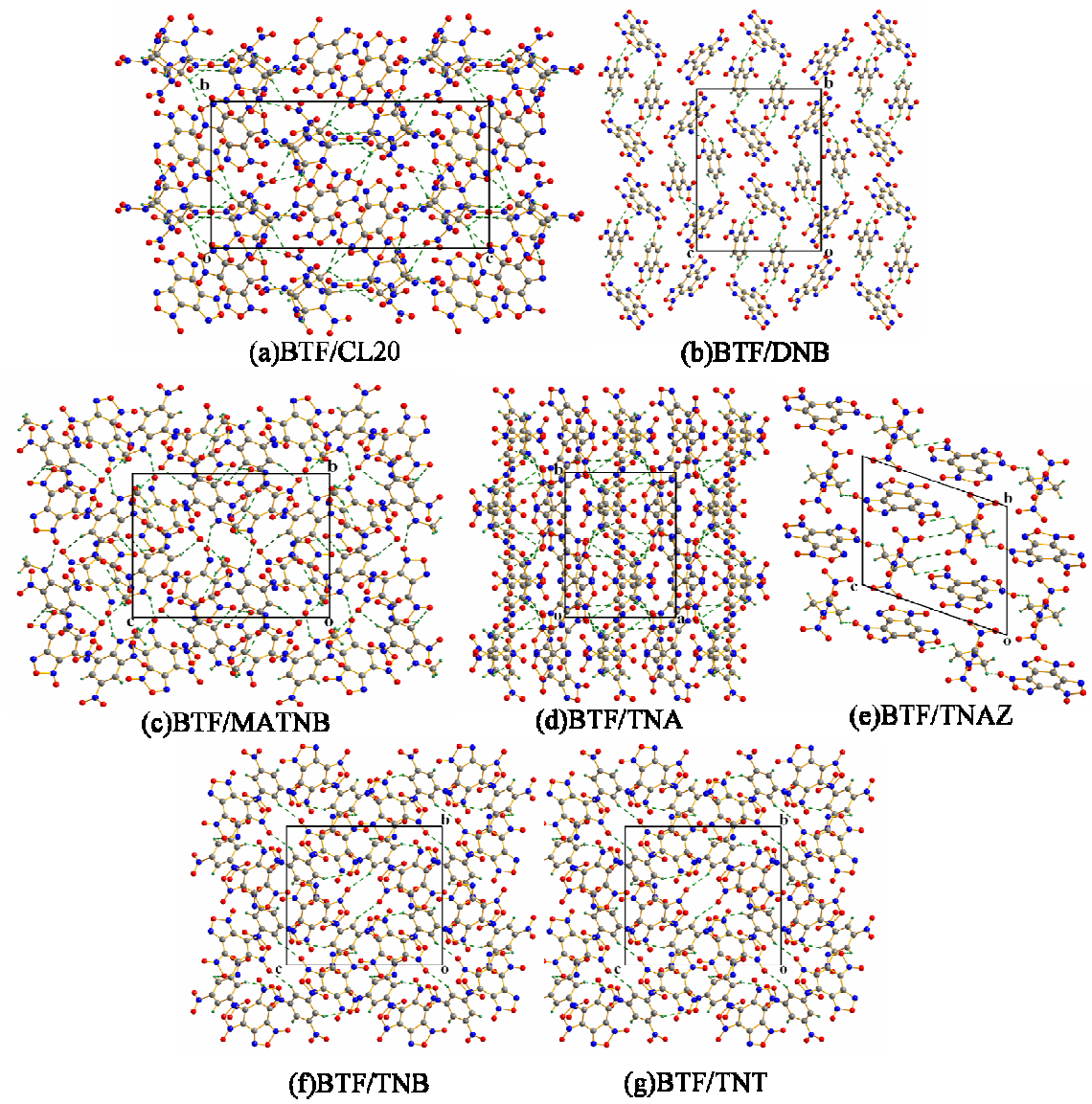

Fig. s1 HBs in the BTF-based EECCs represented by green dash.

CrystEngComm Accepted Manuscript

Table s2. Geometry and QTAIM analyses of the intermolecular HBs in the BTF-based EECCs.

Explosive	Number	D-H, Å	H···A, Å	A···D, Å	A-H···D,°	ρ, e/Å^3	E_{HB}, kJ/mol
BTF/CL-20	a	0.980	2.706	3.595	150.9	0.00540	4.0
	b	0.980	2.766	3.596	142.9	0.00413	3.5
	c	0.980	2.448	3.338	150.7	0.00983	6.8
BTF/DNB	d	0.929	2.468	3.322	152.8	0.00794	6.5
	e	0.930	2.765	3.352	122.0	0.00475	4.0
BTF/MATNB	f	0.881	2.288	3.066	147.3	0.00912	8.3
	g	0.950	2.626	3.525	158.1	0.00570	4.5
	h	0.980	2.555	3.364	139.9	0.00600	5.1
	i	0.950	2.507	3.454	173.9	0.00745	5.8
BTF/TNA	j	0.949	2.782	3.393	122.9	0.00471	4.0
	k	0.949	2.669	3.610	171.4	0.00536	4.1
	l	0.950	2.759	3.684	164.8	0.00433	3.5
	m	0.880	2.440	2.977	119.8	0.00868	7.8
	n	0.880	2.406	3.186	147.9	0.00750	6.5
BTF/TNAZ	o	0.970	2.795	3.405	121.6	0.00444	3.8
	p	0.970	2.795	3.405	121.6	0.00444	3.8
BTF/TNB	q	0.930	2.759	3.397	126.7	0.00487	4.0
	r	0.930	2.743	3.605	154.6	0.00380	3.1
BTF/TNT1	s	0.981	2.569	3.280	129.4	0.00702	5.8
	t	0.950	2.789	3.718	165.9	0.00400	3.2
	u	0.950	2.714	3.375	127.3	0.00533	4.4
BTF/TNT2	v	0.981	2.588	3.402	140.5	0.00790	5.7
	w	0.980	2.568	3.334	135.0	0.00678	5.6
	x	0.950	2.676	3.582	159.7	0.00519	4.2
	y	0.980	2.507	3.175	125.3	0.00783	6.6

CrystEngComm Accepted Manuscript

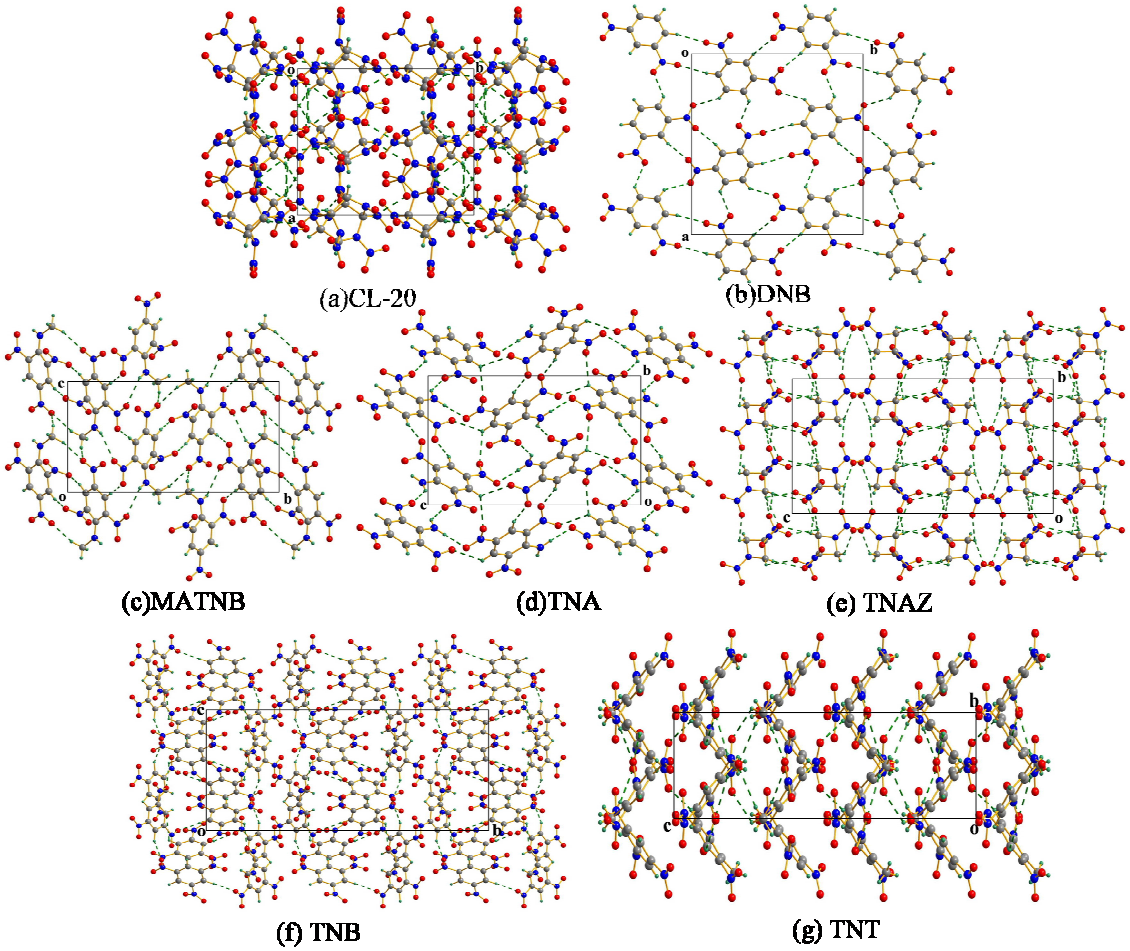

Fig. s2 HBs in the pure coformer crystals represented by green dash.

CrystEngComm Accepted Manuscript

Table s3. Geometry and QTAIM analyses of the intermolecular HBs in pure coformer crystals.

Explosive	Number	D-H, Å	H···A, Å	A···D, Å	A-H···D,º	ρ, e/Å^3	E_{HB}, kJ/mol
CL-20	a1	0.896	2.621	3.177	121.0	0.00762	6.9
	a2	0.809	2.602	3.235	136.3	0.00723	6.0
	a3	0.961	2.660	3.306	124.9	0.00690	5.8
	a4	0.961	2.778	3.277	113.1	0.00591	5.3
	a5	0.961	2.503	3.275	137.3	0.00760	6.2
	a6	0.961	2.767	3.556	139.9	0.00348	2.9
DNB	b1	0.929	2.555	3.267	133.7	0.00722	5.9
	b2	0.930	2.635	3.497	154.3	0.00512	4.1
	b3	0.930	2.632	3.429	144.1	0.00640	5.1
	b4	0.930	2.689	3.573	158.8	0.00477	3.7
MATNB	c1	1.000	2.544	3.420	146.3	0.00755	6.0
	c2	0.942	2.674	3.507	147.7	0.00520	4.1
	c3	0.922	2.562	3.278	134.9	0.00726	6.0
	c4	0.925	2.565	3.136	120.4	0.00696	6.3
	c5	0.861	2.672	3.520	168.4	0.00531	4.0
TNA	d1	0.884	2.359	3.033	133.2	0.01068	9.3
	d2	0.984	2.546	3.245	127.9	0.00762	6.1
	d3	0.984	2.593	3.189	119.1	0.00670	5.6
	d4	0.924	2.379	3.153	135.8	0.00805	7.2
	d5	1.010	2.546	3.523	162.7	0.00589	4.6
TNAZ	e1	0.954	2.706	3.367	127.0	0.00510	4.2
	e2	0.940	2.792	3.731	177.0	0.00405	3.1
	e3	0.940	2.666	3.125	110.8	0.00705	5.9
	e4	1.058	2.676	3.286	116.3	0.00607	5.0
	e5	1.058	2.638	3.464	134.6	0.00668	5.3
	e6	0.940	2.762	3.239	112.4	0.00503	4.3
	e7	0.954	2.696	3.440	135.2	0.00503	4.1
TNB	f1	1.064	2.246	3.294	168.3	0.01169	9.4
	f2	1.165	2.281	3.369	154.3	0.0117	9.4
	f3	1.098	2.629	3.256	115.4	0.00765	6.1
TNT1	g1	1.079	2.540	3.516	150.0	0.00752	5.8
	g2	0.936	2.621	3.307	130.6	0.00614	5.0
	g3	1.083	2.382	3.429	162.2	0.00993	7.6
	g4	0.974	2.784	3.439	125.2	0.00516	4.3
	g5	1.033	2.631	3.347	126.3	0.00779	6.4
TNT2	h1	1.002	2.683	3.390	127.8	0.00557	4.5

CrystEngComm Accepted Manuscript

h2	1.083	2.382	3.429	162.2	0.00993	7.6
h3	0.905	2.613	3.447	153.6	0.00603	4.8
h4	0.983	2.701	3.490	137.5	0.00485	4.1
h5	0.974	2.784	3.439	125.2	0.00516	4.3
h6	1.033	2.631	3.347	126.3	0.00779	6.4

CrystEngComm Accepted Manuscript

S3. Hirshfeld surface of BTF molecules involved in pure BTF crystal and the seven BTF-based EECCs.

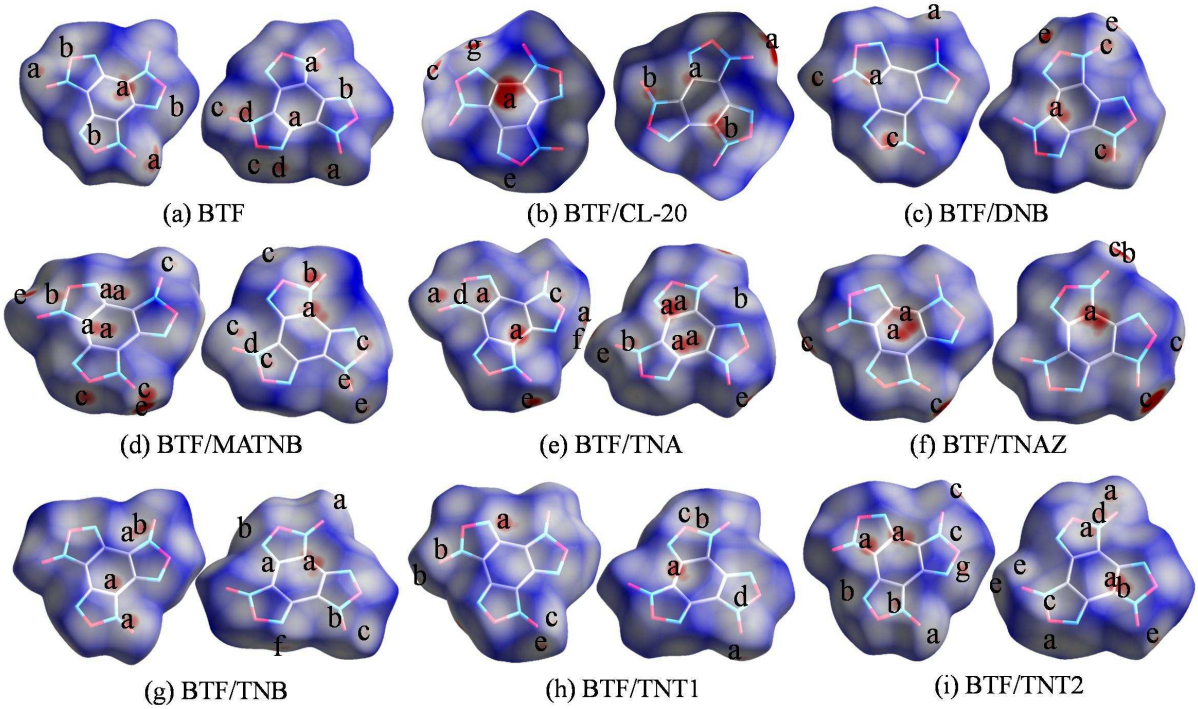

Fig. s3 Hirshfeld surfaces of BTF molecules in crystals, each shows by two plots with a torsion of 180°. Because BTF/TNT has Z′=2, the surfaces are illustrated by (h) and (i) separately. a-g denote the contacts of C···O, N···O, O···O, N···N, O···H, C···N, and N···H, respectively.

S4. References

[1] H. H. Cady, A. C. Larson, D. T. Cromer, *Acta Crystallogr*. **1966**, 20, 336.

[2] Z. Yang, H. Li, X. Zhou, C. Zhang, H. Huang, J. Li, F. Nie, *Cryst. Growth Des.,* **2012**, *12*, 5155.

[3] Z. Yang, Y. Wang, J. Zhou, H. Li, H. Huang, F. Nie, *Propellants Explos. Pyrotech.,* **2014**, *39*, 9.

[4] H. Zhang, C. Guo, X. Wang, J. Xu, X. He, Y. Liu, X. Liu, H. Huang, J. Sun, *Cryst. Growth Des.,* **2013**, *13*, 679.

CrystEngComm Accepted Manuscript